

Implementation of the Statistical Cloud Scheme Option: Preliminary Tests

E. AVGOUSTOGLOU, T. TZEFERI AND I. PAPAGEORGIOU

Hellenic National Meteorological Service, Athens, Greece

1 Introduction

In general, cloud models are implemented in numerical weather prediction with the main assumption that the computational grid volume is either entirely saturated or entirely unsaturated. From a closer physics standpoint, this conjecture might be insufficient since substantial portions of grid volumes contain saturated air near boundaries. Additionally, cumulus interiors may contain unsaturated air due to lateral merging of adjacent clouds and entrainment while the initial stage of cloud growth might be treated incorrectly because no latent heat is released until an entire grid volume is saturated. The complexity of these processes leads to the investigation for possible improvement to the cloud model of LM by deriving dependencies of mean cloud fraction upon humidity statistics by assuming Gaussian quasi-conservative properties (Refs. Betts (1973), Sommeria and Deardorff (1977), Mellor (1977), Mellor and Yamada (1982), Raschendorfer (2005)).

Currently, there are two different schemes for sub-grid scale cloudiness in the LM. A simple one based on relative humidity, and another one, called a statistical cloud scheme, which depends on the statistical properties of the saturation deficit within the turbulence scheme. The first scheme is currently used to feed the radiation scheme with cloud information, and has hence been tuned for this purpose. In addition, its results are used as model output as well. The statistical scheme on the other hand is currently used only within the moist turbulence scheme. As the statistical scheme is more sophisticated, it would be of considerable importance to use only this scheme, both for turbulence and radiation as well as for model output.

2 Analysis

For the implementation of the statistical cloud scheme we follow the works of Sommeria and Deardorf (1977) as well as Mellor (1977) where the subgrid low cloud fraction R and mean liquid water content \bar{q}_l are estimated as

$$R = \int_{-\infty}^{\infty} \int_{-\infty}^{\infty} H(q_w - q_s) G dq_w d\theta_l \quad (1)$$

and

$$\bar{q}_l = \int_{-\infty}^{\infty} \int_{-\infty}^{\infty} (q_w - q_s) H(q_w - q_s) G dq_w d\theta_l \quad (2)$$

where q_w and q_s correspond to the total-water and saturation specific humidities respectively, θ_l is the liquid water potential temperature, H stands for the Heaviside function

$$H = \begin{cases} 0, & x < 0 \\ 1, & x > 0 \end{cases} \quad (3)$$

and G is a bivariate normal function

$$G = \frac{1}{2\pi\sigma_{\theta_l}\sigma_{q_w}(1-r^2)^{\frac{1}{2}}} \exp \left[\frac{-1}{1-r^2} \left(\frac{\theta_l'^2}{2\sigma_{\theta_l}^2} - r \frac{\theta_l'q_w'}{\sigma_{\theta_l}\sigma_{q_w}} + \frac{q_w'^2}{2\sigma_{q_w}^2} \right) \right] \quad (4)$$

with primed quantities defined as $x' \equiv x - \bar{x}$ and the correlation factor $r = \overline{\theta_l'q_w'}/(\sigma_{\theta_l}\sigma_{q_w})$.

By assuming a linear approximation for q_s around the value $\bar{q}_{sl} = q_s(\bar{\theta}_l, \bar{p})$ and with the help of Clausius-Clapeyron equation the expressions for R and \bar{q}_l become

$$R \approx \frac{1}{2} \left[1 + \operatorname{erf} \left(\frac{Q}{\sqrt{2}} \right) \right] \quad (5)$$

$$\bar{q}_l \approx \frac{1}{1 + \beta\bar{q}_{sl}} \left[RQ + \frac{\exp\left(\frac{-Q^2}{2}\right)}{\sqrt{2\pi}} \right] \quad (6)$$

where

$$Q = \frac{\bar{q}_w - \bar{q}_{sl}}{\sigma}, \quad \sigma = (\bar{q}_w^2 + \bar{q}_{sl}^2 - 2\bar{q}_w\bar{q}_{sl})^{\frac{1}{2}}, \quad \beta = 0.622 \frac{L^2}{R_d c_p T_l^2} \quad (7)$$

with T_l standing for the liquid water temperature, L is the latent heat for vaporization, R_d is the gas constant for dry air and c_p is the specific heat at constant pressure.

Sommeria and Deardorff (1977), further approximated R through the linear part of an empirical curve that they drew for R by using an ensemble of 400 bivariate normal distributions

$$R \approx 0.5 \left(1 + \frac{Q}{1.6} \right), \quad 0 \leq R \leq 1 \quad (8)$$

In the statistical cloud scheme implemented in the LM, the low cloud cover is parameterized through a similar relation

$$R \approx A \left(1 + \frac{Q}{B} \right), \quad 0 \leq R \leq 1 \quad (9)$$

The parameters A (cloud cover at saturation) and B (critical value of the saturation deficit) are denoted as $zlc0$ and zq_crit and are tunable in the physical parameterization of LM code.

3 Preliminary Tests

Our investigation regarding the implementation of the statistical cloud scheme for low clouds is focused on the weather situation over Greece on January 2 2005. The analysis charts at 500 and 850 Hpa at 06 UTC (right upper and middle graphs of Fig. 1) show an anticyclonic circulation over the western parts of Greece leading to westerly moving warmer air masses streaming over existing colder ones. In the eastern part of the country, a fainting dynamic activity in reference to a passing “trough” retains a weak northern wind current. The vertical correspondence of the anticyclonic circulation over the western parts of Greece is concluded from the surface analysis chart (lower right graph of Fig. 1). The resulting weak surface winds favor the low cloud development as it is shown on the corresponding infrared satellite picture (Fig. 1).

We present the low and total cloud coverage forecasts at 06 UTC of January 2 2005 from LM Version 3.15 with a 7 kilometer horizontal grid of 35 vertical levels, integration time step of 30 seconds and initial conditions from the DWD global model based on 12 UTC analysis of January 1 2005 (Figs. 2, 3). The rest of the configuration of the LM is described in previous COSMO Newsletters (Avgoustoglou; 2003). The test-runs were performed at the

Test Number	Cloud-Ice	<i>icldm_rad</i>	<i>zq_crit</i>	<i>zlc0</i>	<i>ztkhmin</i>	<i>ztkmmin</i>
1	T	4	4.0	0.5	0	0
2	T	4	4.0	0.5	1	1
3	F	4	4.0	0.5	1	1
4	F	2	4.0	0.5	1	1
5	F	2	6.0	0.5	1	1
6	F	2	2.0	0.5	1	1
7	F	2	6.0	0.8	1	1
8	F	2	2.0	0.8	1	1
9	F	2	6.0	0.2	1	1
10	F	2	2.0	0.2	1	1
11	F	2	4.0	0.8	1	1
12	F	2	4.0	0.2	1	1

Table 1: Combinations of the parameters modified for the considered test runs.

IBM Supercomputing System of the European Center of Medium-Range Weather Forecasts (ECMWF). In addition to the physical parameters modified in order to show the sensitivity of the statistical cloud scheme (i.e. *zlc0* and *zq_crit*), we also performed tests on the cloud-ice scheme impact (Doms, 2002; Doms, 2004) as well as the absolute minimum value diffusion coefficients for heat and momentum (i.e. *ztkhmin*, *ztkmmin*) (Heise, 2005). The parameter choice for the test-runs are presented on Table 1.

4 Results and Conclusions

From the first and second test runs (first and second rows of graphs in Fig. 2), we see that the choice of the minimum value of diffusion coefficients does not effect the low and total cloud cover. The same holds for the inclusion or not of the cloud-ice scheme regarding the simple scheme for cloudiness based on relative humidity (i.e. second and third tests runs referring to the second and third rows of graphs in Fig. 2 respectively). Therefore, the weather situation under study may be considered as particularly suitable regarding isolating the sensitivity of the statistical low cloud cover scheme.

Test runs four to six (Fig. 2) and seven to twelve (Fig. 3) show the response of the low cloud cover to the implementation of the statistical scheme with the parameters *zq_crit* and *zlc0* ranging from 0.8 to 0.2 the former and from 2 to 6 the latter. We tentatively infer that the low cloud cover from the simple scheme for cloudiness (test runs 1-3) as well as test runs 4, 5, 7 and 11 from the statistical cloud scheme give comparable results to the satellite picture. For the test runs where either of the parameters *zq_crit* and *zlc0* take their smallest value (i.e 2 and 0.2 respectively), cloud cover is considerably reduced.

The results, although versatile, look realistic leaving space for further investigation. However, due to the more general impact the statistical cloud scheme may have to the physics of the model, further understanding and testing must be considered before its operational implementation.

References

Betts, A.K., 1973: Non-precipitating cumulus convection and its parameterization. *Quart J. R. Met. Soc.*, 99, pp. 178-196.

Sommeria G. and J. W. Deardorff, 1977: Subgrid-Scale Condensation in Models of Nonprecip-

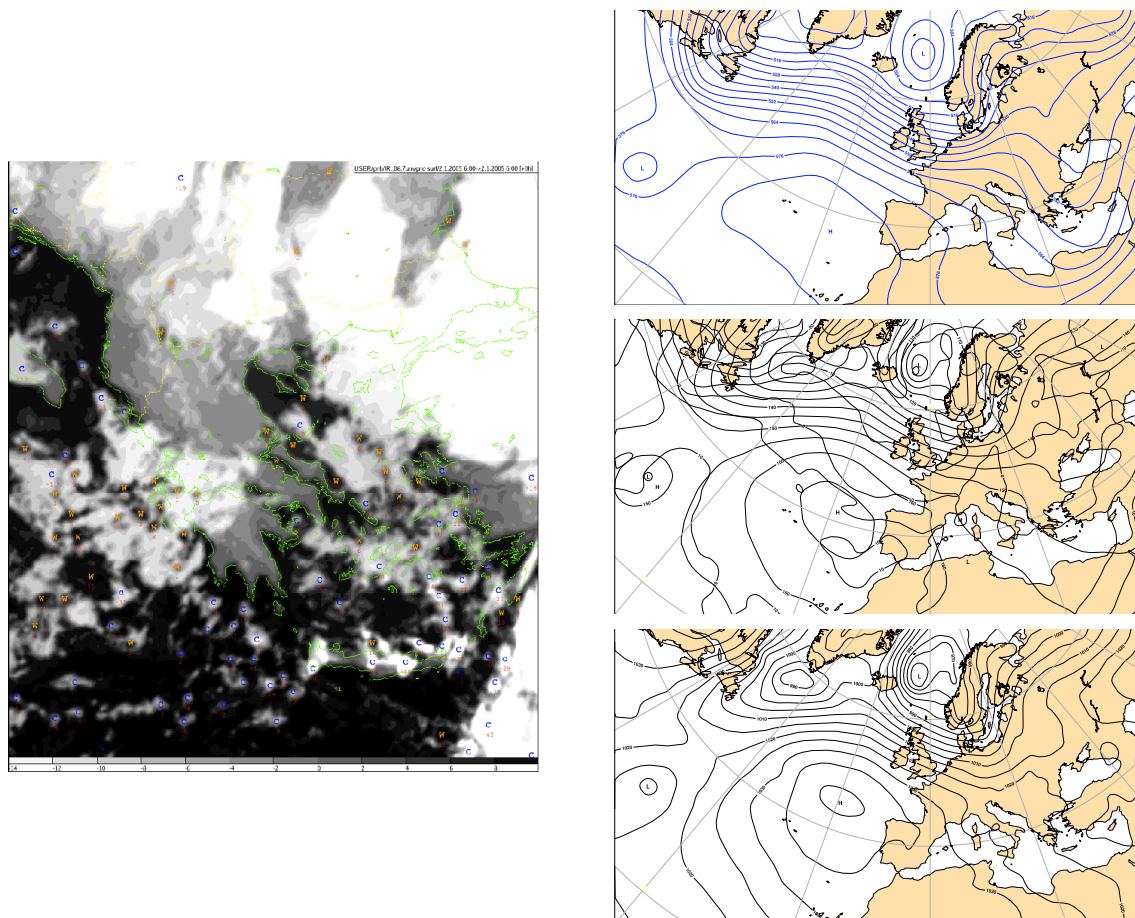


Figure 1: Left: Infrared satellite image, ©METEOSAT. Upper right: Analysis of the geopotential height (meters) for 500 HPa, ©ECMWF. Middle right: Analysis of the geopotential height (meters) and temperature (degrees Celcius) for 850 HPa, ©ECMWF. Lower right: Mean sea level pressure analysis (HPa), ©ECMWF. Date: 2005-01-02:06UTC.

itating clouds. *J. Atmos. Sci.*, 34, pp. 344-355.

Mellor, G.L., 1977: The Gaussian Cloud Model Relations. *J. Atmos. Sci.*, 34, pp. 356-358.

Mellor, G. and T. Yamada, 1982: Development of a Turbulence Closure Model for Geophysical Fluid Problems. *Rev. Geophys. Space Phys.*, 20, pp. 851-875.

Raschendorfer, M., 2005: A new TKE-based Scheme for Vertical Diffusion and Surface-layer Transfer. Deutscher Wetterdienst (DWD), Offenbach and private communication.

Avgoustoglou, E., 2003: Operational Applications of LM at HNMS. *COSMO Newsletter*, No. 3, pp. 28-29.

Doms, G., 2002: The LM cloud ice scheme. *COSMO Newsletter*, No. 2, pp. 128-136.

Doms, G., D. Majewski, A. Müller and B. Ritter, 2004: Recent Changes to the Cloud-Ice scheme. *COSMO Newsletter*, No. 4, pp. 181-188.

Heise, E., 2005: Validation of boundary layer clouds: Test results with the minimum vertical diffusion coefficient set equal to zero in LM. Deutscher Wetterdienst (DWD) and private communication.

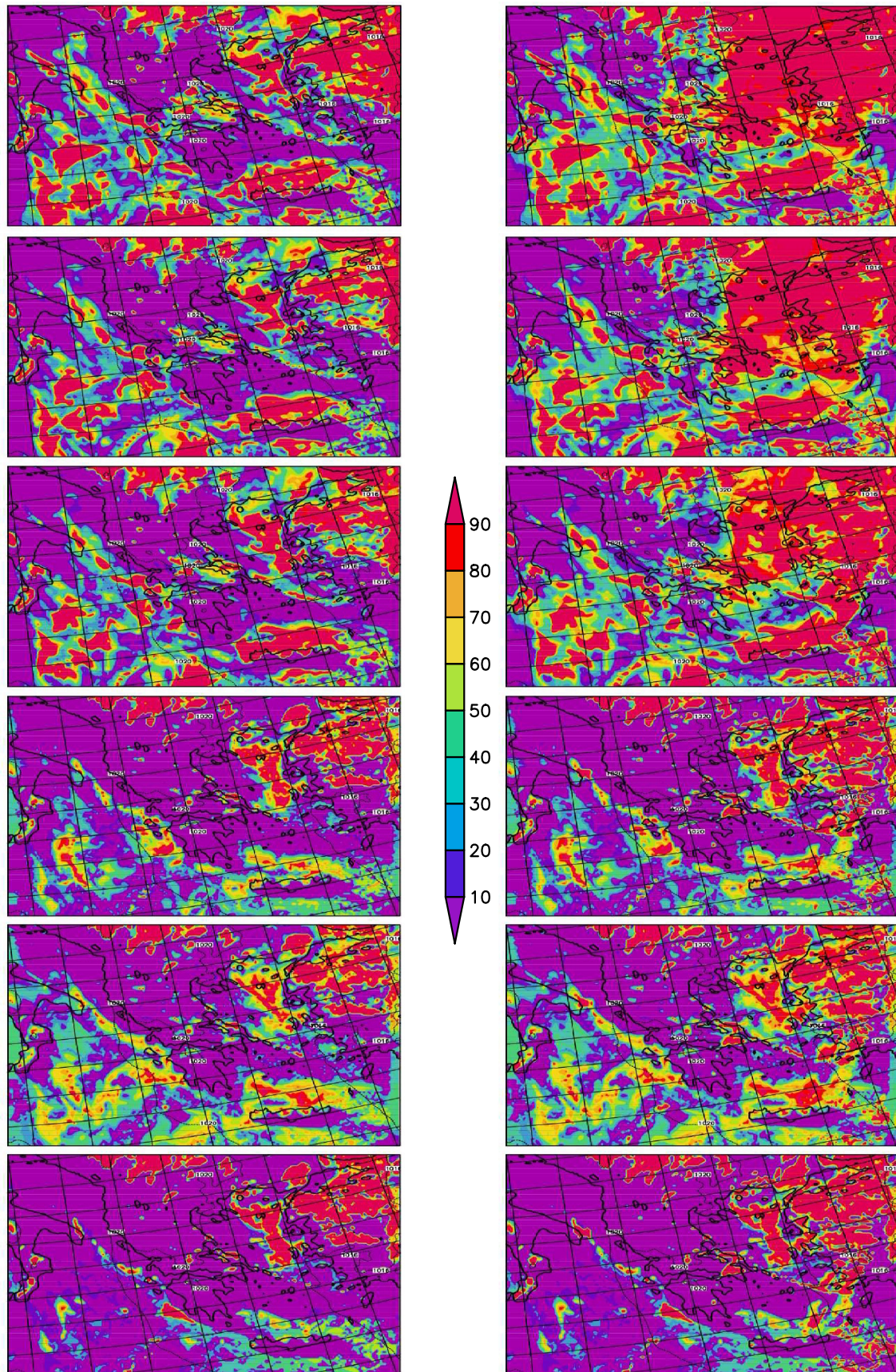


Figure 2: Low (left column) and Total (right column) Cloud Cover forecast (%) and PMSL (HPa), Test Runs No. 1 to No. 6 (from top to bottom) for 2005-01-02:06UTC.

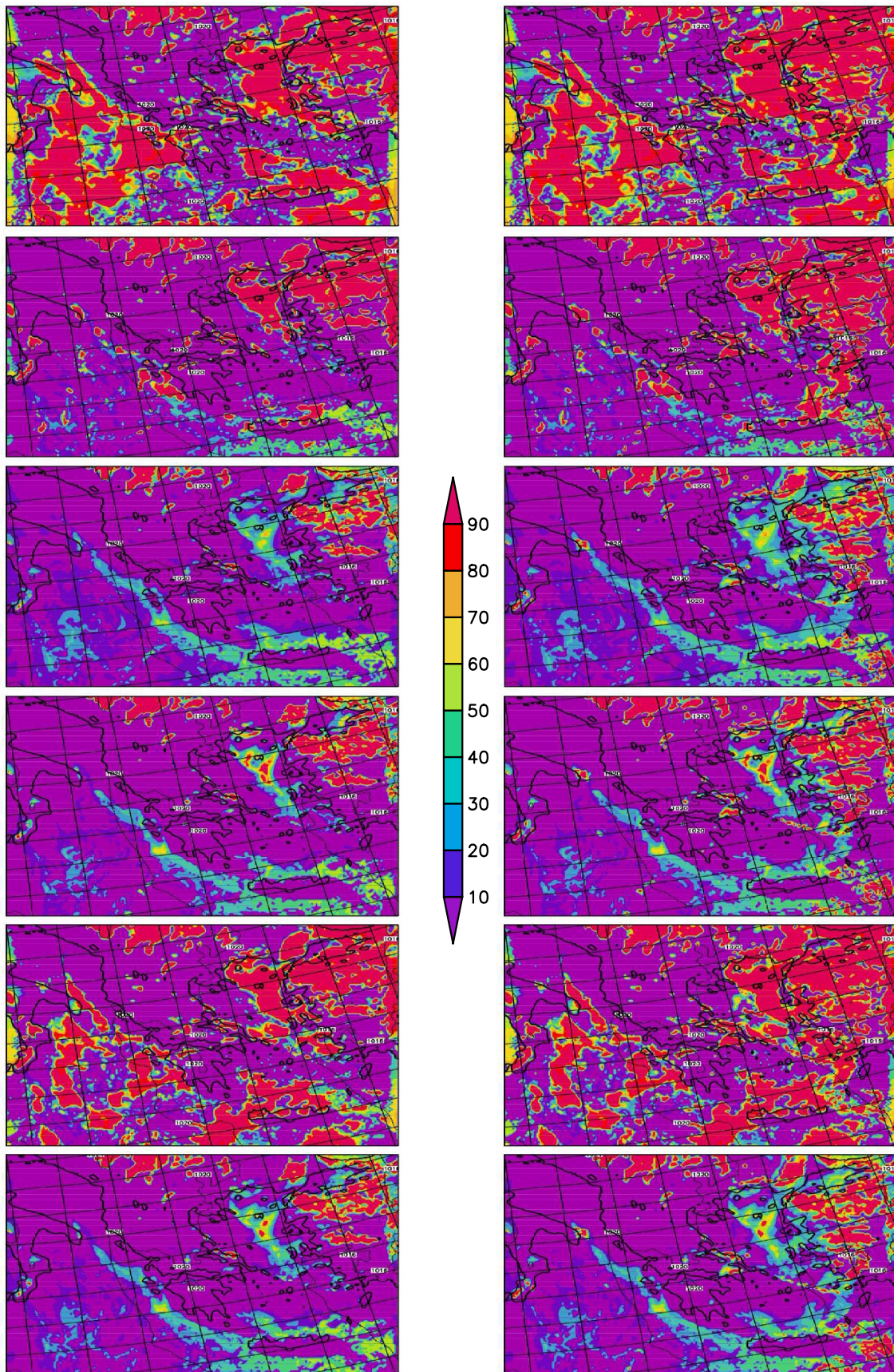


Figure 3: Low (left column) and Total (right column) Cloud Cover forecast (%) and PMSL (HPa), Test Runs No. 7 to No. 12 (from top to bottom) for 2005-01-02:06UTC.